Water Oxidation Reaction

DOI: 10.1002/anie.201407783

Understanding the Role of Gold Nanoparticles in Enhancing the Catalytic Activity of Manganese Oxides in Water Oxidation Reactions**

Chung-Hao Kuo, Weikun Li, Lakshitha Pahalagedara, Abdelhamid M. El-Sawy, David Kriz, Nina Genz, Curtis Guild, Thorsten Ressler, Steven L. Suib, and Jie He**

Abstract: *The Earth-abundant and inexpensive manganese oxides (MnO_x) have emerged as an intriguing type of catalysts for the water oxidation reaction. However, the overall turnover frequencies of MnO_x catalysts are still much lower than that of nanostructured IrO_2 and RuO_2 catalysts. Herein, we demonstrate that doping MnO_x polymorphs with gold nanoparticles (AuNPs) can result in a strong enhancement of catalytic activity for the water oxidation reaction. It is observed that, for the first time, the catalytic activity of MnO_x/AuNPs catalysts correlates strongly with the initial valence of the Mn centers. By promoting the formation of Mn^{3+} species, a small amount of AuNPs (<5%) in α-MnO_2/AuNP catalysts significantly improved the catalytic activity up to 8.2 times in the photochemical and 6 times in the electrochemical system, compared with the activity of pure α-MnO_2.*

The photochemical and electrochemical splitting of water into H_2 and O_2 has received continuous attention over a half century owing to its potential applications in renewable energy technologies. The half-photolysis of the photochemical water oxidation reaction (WOR) and the electrochemical oxygen evolution reaction (OER) $[2H_2O(l) - 4e^- \rightarrow 4H^+(aq) + O_2(g)]$ are known as complex processes involving a four-electron-transfer process. The oxygen generation is kinetically slow and has been recognized as a bottleneck that largely limits the overall efficiency of water splitting. The rational design of numerous novel photochemical and electrochemical catalysts is crucial for more efficient water oxidation.[1] Inspired by highly active cubane-like $CaMn_4O_x$ photocatalysts, researchers have developed the Earth-abundant and inexpensive manganese oxides (MnO_x) as an intriguing type of catalyst for light-driven and electricity-driven water splitting.[2] MnO_x materials have versatile crystalline/amorphous structures due to the multivalent nature of manganese. Given that the complex/variable valence,[2a,3] multiple polymorphs,[1i,4] and versatile morphologies of MnO_x materials[5] can influence their catalytic activity, considerable effort has been devoted to developing highly efficient MnO_x catalysts for water splitting in the past few years. The catalytic activity of MnO_x polymorphs for WORs/OERs is dependent upon the presence of Mn^{3+} species,[6] which have an antibonding electronic configuration and a longer Mn–O bond than that of Mn^{4+}/Mn^{2+} species.[6d]

A number of recent studies have also shown that the underlying substrate (e.g. metal electrode) of the catalysts can significantly improve O_2 evolution performance for both WORs and OERs.[7] The interaction of catalyst and substrate may result in a synergetic coupling effect at their interface, thus leading to the enhancement of catalytic activity.[7g] For instance, Bell's group has demonstrated that cobalt oxide (CoO_x) films deposited on noble metal substrates (e.g. Au, Pt, and Pd) exhibit a much higher activity for OERs.[7b] The turnover frequency (TOF) of CoO_x deposited on Au for OERs is nearly 40 times higher than that of bulk CoO_x. Jaramillo et al. lately reported that the catalytic activity of Au nanoparticle (AuNP) doped MnO_x films was significantly enhanced and that the TOF of AuNPs/MnO_x films was an order of magnitude higher than that of bulk films.[7d] As such, the use of metal oxide catalysts doped with noble metal NPs may stand out as a promising opportunity to develop highly active catalysts for WORs/OERs. However, the underlying role of metal NP dopants in enhancing the catalytic activity for O_2 evolution is still under debate. A study by Primo et al. proposed that the hot electron injection from photoexcited gold NPs (AuNPs) to the catalytic centers may alter the electron-transfer pathways in WORs.[8] One model involves the oxidation of water on the surface of AuNPs. Other reports, conversely, describe the enhanced OER activity of metal oxide catalysts[7b,d] that have core–shell nanostructures[7h] where metal NPs cannot directly interact with water molecules.

[*] C.-H. Kuo, Dr. W. Li, L. Pahalagedara, A. M. El-Sawy, D. Kriz, C. Guild, Prof. S. L. Suib, Prof. J. He
Department of Chemistry, University of Connecticut
Storrs, CT 06269 (USA)
E-mail: steven.suib@uconn.edu
jie.he@uconn.edu
Prof. S. L. Suib, Prof. J. He
Institute of Material Science, University of Connecticut
Storrs, CT 06269 (USA)
N. Genz, Prof. T. Ressler
Department of Chemistry, Technische Universität Berlin
Strasse des 17. Juni 135, 10623 Berlin (Germany)

[**] J.H. acknowledges financial support in the form of startup funds from the University of Connecticut. S.L.S. acknowledges support from the U.S. Department of Energy, Office of Basic Energy Sciences, Division of Chemical, Biological and Geological Sciences (grant DE-FG02-86ER13622A000). We thank Dr. Heng Zhang and Wenqiao Song for assistance with XPS characterization and Prof. Alfredo Angeles-Boza for insightful discussions. This work was supported in part by the Green Emulsions Micelles and Surfactants (GEMS) Center.

Supporting information for this article is available on the WWW under http://dx.doi.org/10.1002/anie.201407783.

In the present study, we focus on five different MnO_x materials doped with AuNPs, i.e., cryptomelane-type α-MnO_2, birnessite-type δ-MnO_2, amorphous MnO_2, cobalt-doped α-MnO_2, and cubic bixbyite Mn_2O_3, to further explore the role of metal NPs on the catalytic activity of MnO_x materials. We observed that, for the first time, the catalytic activity of MnO_x/AuNPs for WORs presented a strong correlation with the valence of Mn centers. For the oxidation state of Mn^{4+}, the MnO_x/AuNPs catalysts (< 5% Au) showed nearly an order of magnitude higher catalytic activity for WORs/OERs than bulk MnO_x catalysts. The electron transfer from Mn^{2+} to AuNPs was envisaged to improve the catalytic activity of MnO_x/AuNPs. Our study highlights the importance of noble metals in developing mixed metal/metal oxide systems as efficient water oxidation catalysts.

Various MnO_x polymorphs were synthesized by following the reported procedures (see the Supporting Information (SI)).[9] AuNPs were deposited on the surface of MnO_x materials through chemical reduction of $HAuCl_4$ using urea. The growth of AuNPs on MnO_x catalysts was confirmed by transmission electron microscopy (TEM) as shown in Figure 1 a, c (for more TEM images see SI). Figure 1 a shows TEM images of as-prepared cryptomelane-type α-MnO_2 nanorods with an average diameter of roughly 20 nm and a length of 200–500 nm. The AuNPs have an average diameter of 4 nm and are well-dispersed on the surface of the α-MnO_2 nanorods. The amount of Au deposited on α-MnO_2 was determined by energy-dispersive X-ray (EDX) spectroscopy. By adjusting the ratio of $HAuCl_4$ and MnO_x, the doping amount of AuNPs could be readily controlled in the range of 0.9% to 5.8% (see Table S1). Catalysts are denoted as MnO_2/AuNP-*n* hereafter, where *n* is the percentage of Au in the catalyst. Other MnO_2 polymorphs, including birnessite-type δ-MnO_2 (Figure 1 c), amorphous MnO_2, cobalt-doped α-MnO_2 rods, and bixbyite Mn_2O_3 (see Figures S6, S8, and S10) were doped with AuNPs using a similar procedure. The crystallinity of MnO_x/AuNP catalysts was further confirmed by X-ray diffraction (XRD) and Raman spectroscopy (see SI). No noticeable change in the crystalline structures of MnO_x polymorphs was observed in any sample after Au deposition. The surface area of MnO_x/AuNPs is close to that of pure MnO_x and no obvious changes were observed.

The catalytic performance of MnO_x polymorphs was first evaluated for WORs as photocatalysts utilizing the well-established $[Ru(bpy)_3]^{2+}$–$S_2O_8^{2-}$ system. The overall photoelectrochemical reaction is given by Equation (1).

$$2\,[Ru(bpy)_3]^{2+} + S_2O_8^{2-} + h\nu \rightarrow 2\,[Ru(bpy)_3]^{3+} + SO_4^{2-} \quad (1)$$

Here $[Ru(bpy)_3]^{2+}$ is a photosensitizer and $S_2O_8^{2-}$ is a sacrificial electron acceptor. The formed $[Ru(bpy)_3]^{3+}$ species can be reduced back to $[Ru(bpy)_3]^{2+}$ by pulling one electron from the catalyst where water molecules lose electrons and are oxidized to form O_2. The O_2 generated in solution upon exposure to visible light ($\lambda > 400$ nm) was measured using a needle-type oxygen microsensor. WOR results obtained using α-MnO_2/AuNPs and δ-MnO_2/AuNPs are presented in Figure 1 b, d. Pure α-MnO_2 exhibited a moderate oxygen evolution rate and the dissolved oxygen content was approximately 0.7 mmol mol^{-1} Mn after 3 min (Figure 1 b); in contrast, pure δ-MnO_2 showed nearly no activity for WORs and no significant oxygen content was detected (below 0.2 mmol mol^{-1} Mn) (Figure 1 d). Similar results were reported by Robinson[6d] and Boppana.[10] The deposition of a small amount of AuNPs on both α-MnO_2 and δ-MnO_2 led to a significantly higher rate of oxygen generation. The dissolved oxygen content increased from 4.0 mmol mol^{-1} Mn for α-MnO_2/AuNP-0.9 to 5.8 mmol mol^{-1} Mn for α-MnO_2/AuNP-4.4 with increased loading of AuNPs on α-MnO_2. The TOF of 1.70×10^{-5} s^{-1} for α-MnO_2/AuNP-4.4 calculated from WOR results is 8.2 times higher than that of pure α-MnO_2 (see Table S2). For δ-MnO_2/AuNPs, a dramatic enhancement of WOR activity was of particular note and the dissolved oxygen content was roughly 18 mmol mol^{-1} Mn. The TOF of δ-MnO_2/AuNP-5.8 is 5.1×10^{-5} s^{-1}, close to that of Mn_2O_3.[2a]

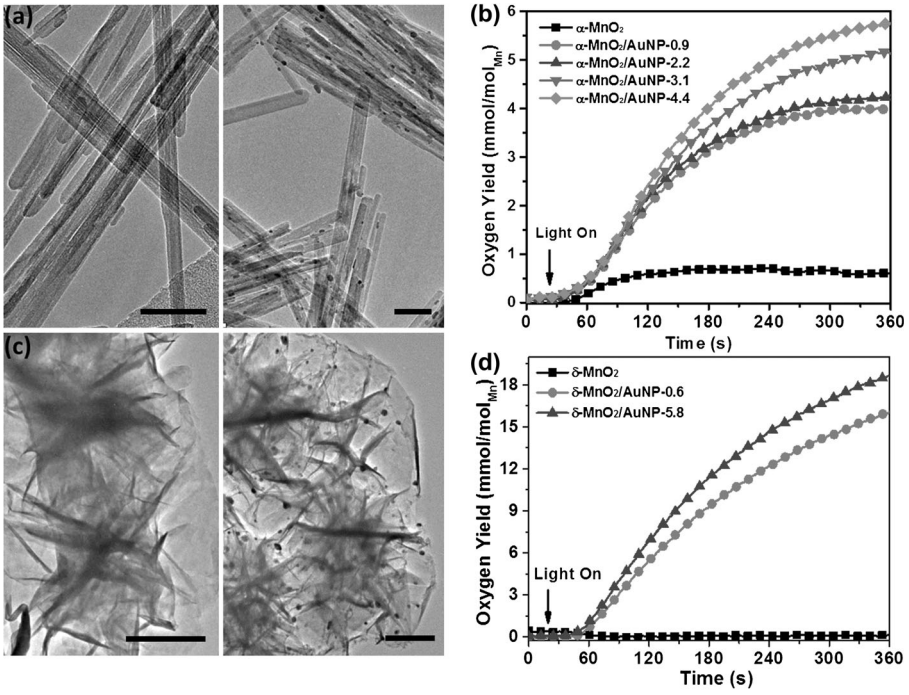

Figure 1. a, c) TEM images of MnO_x (left) and MnO_x/AuNP (right) catalysts: a) α-MnO_2 and α-MnO_2/AuNP-4.4; and c) δ-MnO_2 and δ-MnO_2/AuNP-5.8. Scale bars are 50 nm in (a) and 200 nm in (c). b, d) Concentration of dissolved O_2 measured under visible-light irradiation (> 400 nm) with α-MnO_2/AuNP (b) and δ-MnO_2/AuNP (d) as catalysts. Conditions: 1.5 mM $[Ru(bpy)_3]^{2+}$, 13 mM $Na_2S_2O_8$, 68 mM Na_2SO_4, and 3 mg of catalyst in 15 mL Na_2SiF_6/$NaHCO_3$ buffer solution (pH ≈ 5.8). The WOR results were confirmed by a minimum of three individual measurements.

Likewise, the enhancement of WOR activity was found in the other two types of MnO_2 polymorphs, including amorphous MnO_2 and cobalt-doped α-MnO_2 rods (see Figures S12 and S13). Moreover, the increase of the doping contents of AuNPs in MnO_x polymorphs seemed to further improve the catalytic activity, but this effect is minimal.[11] WOR results suggest that the addition of AuNPs to MnO_x polymorphs results in a much higher photochemical catalytic activity.

To further explore the enhanced catalytic activity of MnO_2/AuNP catalysts, the OER performance of α-MnO_2/AuNP was also evaluated by cyclic voltammetry (CV). The voltammograms of α-MnO_2/AuNPs with various contents of AuNPs under alkaline conditions (0.1 M KOH, pH ≈ 13) are shown in Figure 2 (see SI for details). Larger current density

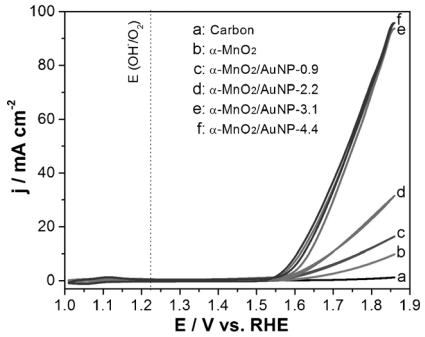

Figure 2. Cyclic voltammetry studies of α-MnO_2 and α-MnO_2/AuNP for the electrochemical oxidation of water. All measurements were carried out in O_2-purged 0.1 M KOH solution at a scan rate of 10 $mV s^{-1}$; rotation rate of 1600 rpm for the rotating disk electrode.

and lower overpotential of water oxidation were obtained with a higher loading of AuNPs. The overpotential (η) at the current density (j) of 10 $mA cm^{-2}$ is 0.39 V for α-MnO_2/AuNP-4.4, compared to pure α-MnO_2 with $\eta = 0.63$ V (Table S2). The mass activity of α-MnO_2/AuNP-4.4 at $\eta =$ 0.35 V is about 6 times higher than that of pure α-MnO_2, while the TOF of α-MnO_2/AuNP-4.4 for OERs is roughly 10 times higher than that of pure α-MnO_2. It is quite challenging to compare the catalytic activity to that of previously published MnO_x catalysts as the sample preparation and measurement conditions vary. However, under similar conditions, Fekete et al. reported the electrochemical activity of nanostructured β-MnO_2 catalysts and found that the overpotential at $j = 10$ $mA cm^{-2}$ is 0.55 V in NaOH solution (0.1 M), which is close to that of pure α-MnO_2 in this work.[12] The recent report from Gorlin and Jaramillo showed that the electrodeposited MnO_x/AuNP composite catalyst has an overpotential of 0.35 V at $j = 10$ $mA cm^{-2}$.[7d] Similar effects from AuNP doping are shown in the study we present here.

How does the intriguing catalytic synergy of MnO_x/AuNPs for water splitting occur? To investigate synergetic effects, it is useful to address two important factors: 1) the influence of AuNPs on the structure and surface properties of MnO_x, including the crystal structures of MnO_x and the valence/oxidation state of Mn; and 2) the influence of AuNPs on the reaction pathways and catalytic centers, for example, whether AuNPs can act as co-catalysts or new active centers instead of Mn. As previously mentioned, macroscopic crystalline structures of MnO_x catalysts were not influenced by the presence of AuNPs. The enhancement of WORs may be ascribed to the change in either the surface properties of the MnO_2/AuNP catalysts or the in situ involvement of AuNPs in the WOR mechanism.

The surface properties of MnO_2/AuNPs catalysts were first investigated by X-ray photoelectron spectroscopy (XPS). The high-resolution XPS spectra of the Mn 2p region (Figure S15) present two peaks at 642.2 eV and 653.8 eV assigned to Mn $2p_{3/2}$ and $2p_{1/2}$, respectively. The difference in the binding energy of the two peaks, which is frequently used for characterizing Mn^{3+} and Mn^{4+} ratios, did not display any significant change compared to that of pure α-MnO_2. However, the Mn K-edge X-ray absorption near-edge structure (XANES) analysis of MnO_2/AuNPs catalysts suggested a slight change in the average oxidation state of Mn (Figure 3). The overall features of Mn K-edge XANES

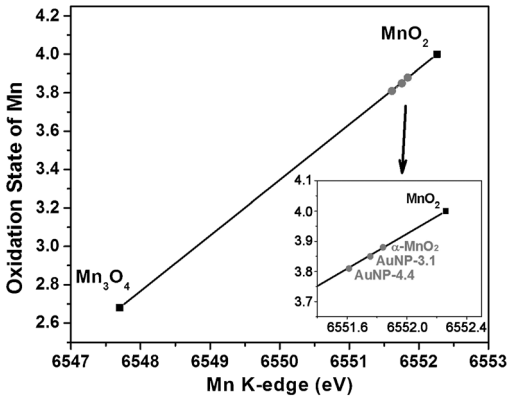

Figure 3. The average oxidation state of Mn for α-MnO_2 and α-MnO_2/AuNP catalysts derived from Mn K-edge absorption threshold.

spectra are quite similar for all samples of α-MnO_2/AuNP. Extended X-ray absorption fine structure (EXAFS) spectra also revealed no significant influence of gold loading on the average Mn–O and Mn–Mn distances (Table S6). However, a decreasing XAFS amplitude indicated an increasing distribution of Mn–O and Mn–Mn distances with gold loading. The slight shift from 6551.84 (α-MnO_2) to 6551.61 eV (α-MnO_2/AuNP-4.4) corresponds to the decrease of the Mn oxidation state from 3.91 (α-MnO_2) to 3.84 (α-MnO_2/AuNP-4.4).[7d] This small shift in binding energy indicates that: 1) the localized electronic interaction of MnO_2 and AuNPs lowers Mn valence; and 2) the weak, positive charge of AuNPs will compensate the change in the valence of Mn, resulting in the formation of Mn species with a lower oxidation state.[13] The co-presence of positive Au ions (Au^{3+}) was further confirmed by Au 4f XPS spectra (Figure S16).

To explore the influence of AuNPs on the reaction pathway and catalytic centers, more control experiments were performed. First, the individual AuNPs (citrate-stabilized AuNPs, 3–5 nm in diameter) were tested for WORs and no oxygen was detected. Second, physically mixing AuNPs

and α-MnO_2 did not enhance the catalytic activity relative to that of pure α-MnO_2. Third, the catalytic performance of Mn_2O_3 and Mn_2O_3/AuNPs catalysts for WORs was examined using the conditions identical to those of the $[Ru(bpy)_3]^{2+}$–$S_2O_8^{2-}$ system (see Figure 4). There is no significant difference in the catalytic activity of Mn_2O_3, Mn_2O_3/AuNP-0.4, and Mn_2O_3/AuNP-3.9 catalysts for WORs. The TOF value of $4.39\times10^{-5}\ s^{-1}$ for Mn_2O_3 is close to that of Mn_2O_3/AuNPs, $4.14\times10^{-5}\ s^{-1}$ (within 5%). We can conclude from these results: 1) AuNPs are catalytically "inactive" for WORs in the absence of MnO_2 catalysts in the photochemical system; 2) the mixture of AuNPs with MnO_2 did not promote the activity of MnO_2, indicating that the interaction of AuNPs and MnO_2 is localized and diminished at long distance; and 3) the deposition of AuNPs on Mn_2O_3 does not improve its WOR activity, implying that only Mn^{3+} species are the catalytic centers and AuNPs are not directly involved in the WORs. This suggests that AuNPs cannot act as the catalytic centers for WORs or modify the electron-transfer pathways between the water molecules and the catalytic centers.

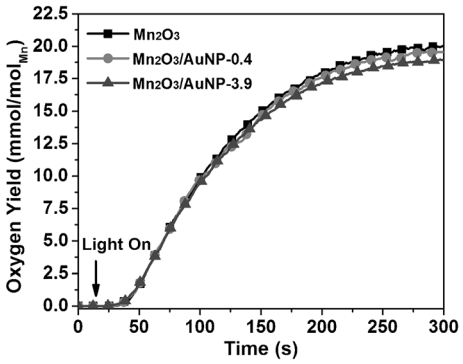

Figure 4. Concentration of dissolved O_2 generated with Mn_2O_3 and Mn_2O_3/AuNPs catalysts under visible-light irradiation (>400 nm).

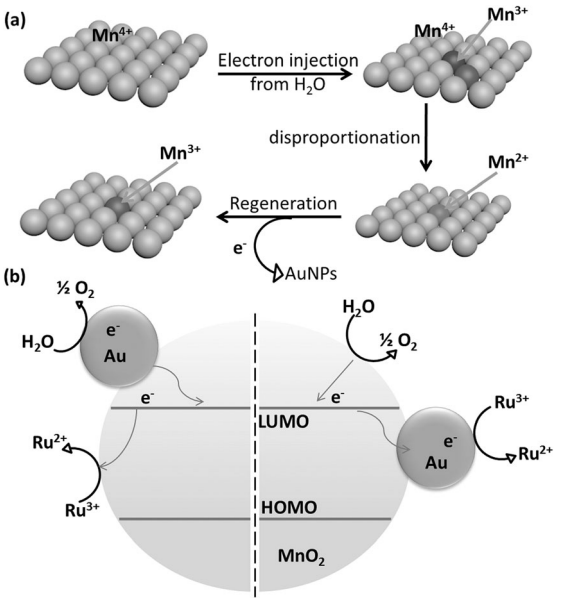

Scheme 1. a) The changes in the oxidation state of Mn catalytic centers in the photochemical water oxidation. b) Schematic illustration of the mechanism for photochemical water oxidation with the $[Ru(bpy)_3]^{2+}$–$S_2O_8^{2-}$ system on MnO_x/AuNPs catalysts. The proposed electron-transfer pathways describe two possibilities involving oxidation of water (loss of an electron) on AuNPs (left) or on MnO_2 (right).

In general, Mn^{3+} species have a very labile Mn–O bond compared to that of Mn^{4+}/Mn^{2+} species and it can act as precursors for O_2 evolution. The active Mn^{3+} species can be generated by the electron injection from H_2O to Mn^{4+} ions in MnO_2.[6b] However, they are rather unstable under natural or acidic conditions, and the disproportionation of Mn^{3+} to Mn^{2+} and Mn^{4+} species occurs quickly to diminish the active Mn^{3+} centers for WORs (Scheme 1a, $2Mn^{3+}\rightarrow Mn^{2+}+Mn^{4+}$). The equilibrium concentration of Mn^{3+} species is less than 10^{-14}% of the initial concentration of Mn^{4+} and Mn^{2+} at pH ≈ 6.[6b] Based on our observation of valence-dependent catalytic activity, it is reasonable to deduce that AuNPs in MnO_2/AuNPs catalysts promote the in situ formation of active Mn^{3+} species for WORs. One hypothesis is that the loss of an electron from the Mn^{2+} species to AuNPs through the reaction $2Mn^{2+}+3H_2O\rightarrow Mn_2O_3+2e^-+6H^+$ regenerates Mn^{3+} catalytic centers (Scheme 1a). In this redox reaction, the electron transfer from Mn^{2+}/Mn^{3+} ($E^o=+1.49$ V) redox pairs to AuNPs (note that, for Au^+/Au $E^o=+1.83$ V and for Au^{3+}/Au $E^o=+1.52$ V) continuously yields Mn^{3+} species. The results presented in Figure 3 clearly demonstrate that the localized electronic interaction of MnO_2 and AuNPs leads to the weakly positive charge. The electron-transfer pathway will increase the concentration of surface Mn^{3+} species, but not directly impact the loss of electrons from the water molecules. For Mn_2O_3 catalysts, Mn^{3+} species preexist; thus, no change in activity of Mn_2O_3/AuNP catalysts was observed. Moreover, the electronic communication of AuNPs and other metal oxide semiconductors has been reported previously at a metal–semiconductor interfaces, for example, AuNPs/TiO_2[14] and AuNPs/WO_3.[15] AuNPs may also increase the electron-transfer efficiency at the metal–semiconductor interface,[14b] compared to catalytic materials and Ru^{2+}/Ru^{3+} redox species.

We have examined the in situ change of the oxidation state of Mn species using UV/Vis spectroscopy. As shown in Figure 5a, α-MnO_2 displayed a broad peak centered at 370 nm in aqueous solution, corresponding to the d–d transition band gap of MnO_2.[16] The broadness of the absorption peak is due to the coexistence of lower oxidation states of Mn in α-MnO_2.[6a] For instance, Mn^{3+} species in the octahedral center induce a red-shift of the absorption band due to the single spin-allowed d–d transition and the charge transfer between Mn^{3+} and O.[16b] The change in the spectra of α-MnO_2/AuNP-4.4 catalysts (0.1 mg mL^{-1}) was recorded in the presence of $Na_2S_2O_8$ as an electron acceptor at a time interval of 1 min (Figure 5a). The gradual red-shift of the absorption peak (≈50 nm) of α-MnO_2 to a longer wavelength occurs with increasing reaction time. The change in the absorption of α-MnO_2 as a function of reaction time is plotted in Figure 5b. The new peak appearing at 540–560 nm is ascribed to the generation of surface Mn^{3+} species. The control experiments were performed with pure α-MnO_2

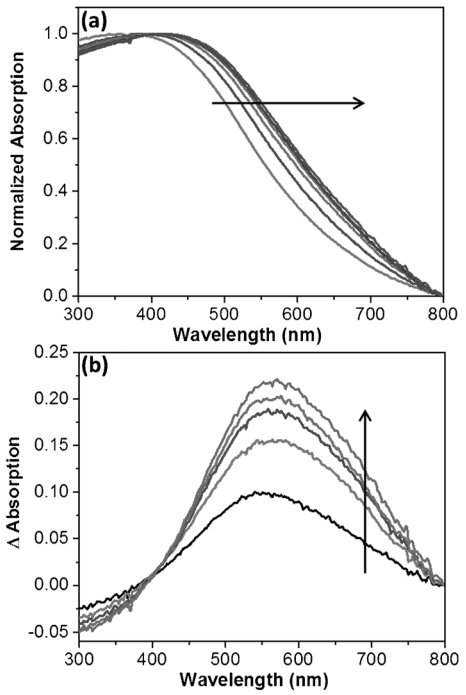

Figure 5. a) Time-resolved UV/Vis absorption spectra of α-MnO_2/AuNP-4 (0.1 mg mL^{-1}) in the presence of $Na_2S_2O_8$. The absorption spectra were measured immediately after the addition of $Na_2S_2O_8$ and at regular time intervals of 1 min. b) Changes in the UV/Vis absorption of α-MnO_2/AuNP-4.4 over 6 min after subtracting the reference spectrum recorded at $t = 1$ min. The arrows indicate the increase of reaction time.

without AuNPs and α-MnO_2 mixed with free AuNPs under identical conditions (Figure S17). No absorption shift was observed in these experiments.

The changes in the spectra of α-MnO_2/AuNP-4.4 suggest that AuNPs promote the formation of active Mn^{3+} species. The electron transfer between Mn and $S_2O_8^{2-}$ is known to be thermodynamically favorable ($S_2O_8^{2-}/SO_4^{2-}$ $E^o = 2.1$ V) but proceeds slowly. The redox reaction cannot be measured in the absence of AuNPs. The role of AuNPs is likely to enhance the electronic communication between Mn and the redox species, for example $S_2O_8^{2-}/SO_4^{2-}$ and Ru^{2+}/Ru^{3+}, by pulling electrons from the catalysts (Scheme 1 b). Similar results were reported in OERs using metal oxides (Co and Ni) with noble metals, where the noble metals generated and stabilized metal ions at higher oxidation states (e.g. Co^{4+} and Ni^{3+}). Such species are recognized as active centers for the water oxidation reaction. Of greater relevance to our present study, Casella et al.[17] and Yeo et al.[7f] demonstrated that the growth of Ni hydroxide on a gold electrode favors the oxide of Ni^{3+} over Ni^{2+}. Yeo et al. also noted that the cobalt oxide deposited on Au electrodes exhibits a high occurrence of Co^{4+} species on the surface.[7b] The enhanced activity was correlated to the electronegativity of noble metals.

In summary, we have systematically studied five different MnO_x/AuNP catalysts in both WORs and OERs. The enhanced catalytic activity of MnO_x after deposition of AuNPs has been confirmed in both photochemical and electrochemical systems. A small amount of AuNPs (< 5 %) served as a dopant and the catalytic activity of α-MnO_2/AuNP was significantly enhanced up to 8.2 times in the photochemical and 6 times in the electrochemical system compared to that of pure α-MnO_2. The catalytic activity of MnO_x/AuNPs was found to be strongly correlated to the valence of Mn centers. The enhanced electronic communication between Mn and the redox species that solely promotes the in situ formation of active Mn^{3+} species for WORs played a key role in the increased catalytic activity of MnO_2/AuNPs. Our results may provide fundamental guidance in the preparation of highly active transition-metal oxide catalysts for both WORs and OERs.

Received: July 31, 2014
Published online: October 3, 2014

Keywords: manganese oxide · metal nanoparticles · oxygen evolution reaction · transition-metal oxides · water oxidation

[1] a) M. Bajdich, M. García-Mota, A. Vojvodic, J. K. Nørskov, A. T. Bell, *J. Am. Chem. Soc.* **2013**, *135*, 13521 – 13530; b) R. Subbaraman, D. Tripkovic, K.-C. Chang, D. Strmcnik, A. P. Paulikas, P. Hirunsit, M. Chan, J. Greeley, V. Stamenkovic, N. M. Markovic, *Nat. Mater.* **2012**, *11*, 550 – 557; c) J. Rosen, G. S. Hutchings, F. Jiao, *J. Am. Chem. Soc.* **2013**, *135*, 4516 – 4521; d) F. Jiao, H. Frei, *Angew. Chem. Int. Ed.* **2009**, *48*, 1841 – 1844; *Angew. Chem.* **2009**, *121*, 1873 – 1876; e) Q. Yin, J. M. Tan, C. Besson, Y. V. Geletii, D. G. Musaev, A. E. Kuznetsov, Z. Luo, K. I. Hardcastle, C. L. Hill, *Science* **2010**, *328*, 342 – 345; f) M. W. Kanan, D. G. Nocera, *Science* **2008**, *321*, 1072 – 1075; g) D. M. Robinson, Y. B. Go, M. Greenblatt, G. C. Dismukes, *J. Am. Chem. Soc.* **2010**, *132*, 11467 – 11469.

[2] a) M. M. Najafpour, T. Ehrenberg, M. Wiechen, P. Kurz, *Angew. Chem. Int. Ed.* **2010**, *49*, 2233 – 2237; *Angew. Chem.* **2010**, *122*, 2281 – 2285; b) J. Yano, J. Kern, K. Sauer, M. J. Latimer, Y. Pushkar, J. Biesiadka, B. Loll, W. Saenger, J. Messinger, A. Zouni, *Science* **2006**, *314*, 821 – 825.

[3] a) I. Zaharieva, P. Chernev, M. Risch, K. Klingan, M. Kohlhoff, A. Fischer, H. Dau, *Energy Environ. Sci.* **2012**, *5*, 7081 – 7089; b) A. Yamaguchi, R. Inuzuka, T. Takashima, T. Hayashi, K. Hashimoto, R. Nakamura, *Nat. Commun.* **2014**, *5*, 4256.

[4] F. Zhou, A. Izgorodin, R. K. Hocking, V. Armel, L. Spiccia, D. R. MacFarlane, *ChemSusChem* **2013**, *6*, 643 – 651.

[5] F. Zhou, A. Izgorodin, R. K. Hocking, L. Spiccia, D. R. MacFarlane, *Adv. Energy Mater.* **2012**, *2*, 1013 – 1021.

[6] a) A. Iyer, J. Del-Pilar, C. K. King'ondu, E. Kissel, H. F. Garces, H. Huang, A. M. El-Sawy, P. K. Dutta, S. L. Suib, *J. Phys. Chem. C* **2012**, *116*, 6474 – 6483; b) T. Takashima, K. Hashimoto, R. Nakamura, *J. Am. Chem. Soc.* **2012**, *134*, 1519 – 1527; c) T. Takashima, K. Hashimoto, R. Nakamura, *J. Am. Chem. Soc.* **2012**, *134*, 18153 – 18156; d) D. M. Robinson, Y. B. Go, M. Mui, G. Gardner, Z. J. Zhang, D. Mastrogiovanni, E. Garfunkel, J. Li, M. Greenblatt, G. C. Dismukes, *J. Am. Chem. Soc.* **2013**, *135*, 3494 – 3501.

[7] a) M. R. Gao, Y. F. Xu, J. Jiang, Y. R. Zheng, S. H. Yu, *J. Am. Chem. Soc.* **2012**, *134*, 2930 – 2933; b) B. S. Yeo, A. T. Bell, *J. Am. Chem. Soc.* **2011**, *133*, 5587 – 5593; c) S. Yusuf, F. Jiao, *ACS Catal.* **2012**, *2*, 2753 – 2760; d) Y. Gorlin, C. J. Chung, J. D. Benck, D. Nordlund, L. Seitz, T. C. Weng, D. Sokaras, B. M. Clemens, T. F. Jaramillo, *J. Am. Chem. Soc.* **2014**, *136*, 4920 – 4926; e) M. S. El-Deab, M. I. Awad, A. M. Mohammad, T. Ohsaka, *Electrochem. Commun.* **2007**, *9*, 2082 – 2087; f) B. S. Yeo, A. T. Bell, *J. Phys. Chem. C* **2012**, *116*, 8394 – 8400; g) Y. Y. Liang, Y. G. Li, H. L.

Wang, J. G. Zhou, J. Wang, T. Regier, H. J. Dai, *Nat. Mater.* **2011**, *10*, 780 – 786; h) Z. Zhuang, W. Sheng, Y. Yan, *Adv. Mater.* **2014**, *26*, 3950 – 3955.

[8] A. Primo, T. Marino, A. Corma, R. Molinari, H. Garcia, *J. Am. Chem. Soc.* **2011**, *133*, 6930 – 6933.

[9] a) H. Cao, S. L. Suib, *J. Am. Chem. Soc.* **1994**, *116*, 5334 – 5342; b) Q. Gao, O. Giraldo, W. Tong, S. L. Suib, *Chem. Mater.* **2001**, *13*, 778 – 786.

[10] V. B. R. Boppana, F. Jiao, *Chem. Commun.* **2011**, *47*, 8973 – 8975.

[11] L. Trotochaud, S. L. Young, J. K. Ranney, S. W. Boettcher, *J. Am. Chem. Soc.* **2014**, *136*, 6744 – 6753.

[12] M. Fekete, R. K. Hocking, S. L. Y. Chang, C. Italiano, A. F. Patti, F. Arena, L. Spicci, *Energy Environ. Sci.* **2013**, *6*, 2222 – 2232.

[13] A. K. Sinha, K. Suzuki, M. Takahara, H. Azuma, T. Nonaka, K. Fukumoto, *Angew. Chem. Int. Ed.* **2007**, *46*, 2891 – 2894; *Angew. Chem.* **2007**, *119*, 2949 – 2952.

[14] a) J. J. Zhao, C. R. Bradbury, D. J. Fermin, *J. Phys. Chem. C* **2008**, *112*, 6832 – 6841; b) J. N. Chazalviel, P. Allongue, *J. Am. Chem. Soc.* **2011**, *133*, 762 – 764; c) A. Furube, L. Du, K. Hara, R. Katoh, M. Tachiya, *J. Am. Chem. Soc.* **2007**, *129*, 14852 – 14853.

[15] A. Tanaka, K. Hashimoto, H. Kominami, *J. Am. Chem. Soc.* **2014**, *136*, 586 – 589.

[16] a) Y. Omomo, T. Sasaki, L. Z. Wang, M. Watanabe, *J. Am. Chem. Soc.* **2003**, *125*, 3568 – 3575; b) F. Milella, J. M. Gallardo-Amores, M. Baldi, G. Busca, *J. Mater. Chem.* **1998**, *8*, 2525 – 2531.

[17] I. G. Casella, M. R. Guascito, M. G. Sannazzaro, *J. Electroanal. Chem.* **1999**, *462*, 202 – 210.

